ELSEVIER SCIENCE Inc. [DTD 4.1.0]
JOURNAL ADWR ARTICLE No. 383
PAGES 1-12 DISPATCH 31 October 2000
ADWR 383
PROD. TYPE: FROM DISK
A

ELSEVIER

Advances in Water Resources

Advances in Water Resources 000 (2000) 000–000

www.elsevier.com/locate/advwatres

Simultaneous scaling of soil water retention and unsaturated hydraulic conductivity functions assuming lognormal pore-size distribution

A. Tuli [a], K. Kosugi [b], J.W. Hopmans [a,*]

[a] *Hydrology Program, Department of Land, Air and Water Resources, University of California, Davis, CA 95616, USA*
[b] *Laboratory of Erosion Control, Graduate School of Agriculture, Kyoto University, Kyoto 606-8502, Japan*

Abstract

Using simultaneous scaling, soil spatial variability of hydraulic functions can be described from a single set of scaling factors. The conventional scaling approach is based on empirical curve fitting, without paying much attention to the physical significance of the scaling factors. In this study, the concept of simultaneous scaling of the soil water retention and unsaturated hydraulic conductivity functions is applied to a physically based scaling theory. In this approach, it is assumed that soils are characterized by a lognormal pore-size distribution, which leads directly to lognormally distributed scaling factors. To test this concept, a total of 143 undisturbed soil samples were collected from two soil depths (25 and 50 cm), with each depth divided into two subsets based on the median soil capillary pressure head value, as determined from the lognormal pore-size distribution assumption. Moreover, the theory was compared with the conventional simultaneous scaling method. Both the conventional and physically based simultaneous scaling method performed equally well for all four subsets, as determined from the reduction in weighted root mean squared residual (WRMSR) values after scaling. We showed that the theoretical interpretation of the lognormal scaling factor distribution was applicable to simultaneous scaling of soil hydraulic functions.

Keywords: Scaling; Soil water retention curve; Unsaturated hydraulic conductivity; Lognormal pore-size distribution

1. Introduction

Most of the uncertainty in the assessment of water flow in unsaturated soils at the field scale can be attributed to soil spatial variability as caused by soil heterogeneity. The knowledge of the constitutive relationships for the unsaturated hydraulic conductivity, water saturation, and soil water matric potential are essentially required to study water flow as described by the traditional Richards equation. The exact nature of the functional dependence of these flow variables with water content differs among soil types with different particle size compositions and pore-size geometry within a heterogeneous field soil. This medium-specific character of soil hydraulic functions can be described by soil hydraulic parameters, so that spatially variable soil hydraulic functions are described by spatially variable soil hydraulic parameters.

The scaling approach has been extensively used to characterize soil hydraulic spatial variability and to develop a standard methodology to assess the variability of soil hydraulic functions and their parameters [20,25,32,33]. The single objective of scaling is to coalesce a set of functional relationships into a single curve using scaling factors that describes the set as a whole. The concept of this approach has been developed principally from the theory of microscopic geometric similitude as proposed by Miller and Miller [17]. The procedure consists of using scaling factors to relate the hydraulic properties in a given location to the mean properties at an arbitrary reference point.

Various studies [1,8,16,24] emphasized that scaling of different soil properties for the same field may result in different statistical properties for each of the computed scaling factor distributions, as for the independent scaling of soil water retention and hydraulic conductivity curves. For example, it has been shown that scale factors for soil water retention and unsaturated hy-

* Corresponding author. Tel.: +61-07-4753-8564; fax: +61-07-4753-8600.
E-mail addresses: amtuli@ucdavis.edu (A. Tuli), kos@kais.kyoto-u.ac.jp (K. Kosugi), jwhopmans@ucdavis.edu (J.W. Hopmans).

0309-1708/00/$ - see front matter
PII: S0309-1708(00)00070-1

draulic conductivity functions are not necessarily identical [31,22]. However, at the same time it was emphasized that the ability to characterize all soil hydraulic functions by a single set of scaling factors is highly desirable when simulating and predicting water flow in spatially variable field soils. Moreover, while adopting the similar media concept, equality of scaling factors of soil water retention and unsaturated hydraulic conductivity functions is expected based on the validity of the capillary and Poiseuille equations. Early scaling studies [22,23,31] used an empirical scaling approach, defined as functional normalization, where regression analysis was applied to either soil water retention or unsaturated hydraulic conductivity data [27]. Alternatively, Clausnitzer et al. [4] introduced a scaling method whereby both hydraulic functions were scaled simultaneously using the conventional fitting approach, yielding a single set of scale factors without consideration of the physical significance of the resulting set of scaling factors. Meanwhile, it was shown that scaling factors are log normally distributed, as has also been demonstrated by many others [12,16,31,37].

Difficulties in applying classical Miller similitude scaling to soils with a broad range of particle size distributions and non-uniform porosity has resulted in the development of generalized scaling analysis [24,26], wherein pore-size distribution is considered the invariant soil quantity. Hence, using this approach, the characteristic length is associated with pore space (pore size) rather than the geometric arrangement of both pore space and solid matrix, leading to degree of water saturation, $S = \theta/\theta_s$, as an additional scaling factor [24] for field studies. This approach leads to correlated scaling factor values between those computed from retention and unsaturated hydraulic conductivity functions, which are identical only if soils have identical porosities (geometric similitude scaling).

Recently, the pore radius, r, was used as the microscopic characteristic length to scale soil water retention curves for soils that are characterized by a lognormal pore-size distribution [14]. In their study, the physically based scale factors were computed directly from the physically based parameters describing the individual soil water retention functions [13]. In a subsequent study [9], the physically based scaling theory was applied to both soil water retention and unsaturated hydraulic conductivity data for a forested hill slope soil.

The objective of this study was to extend the physically based scaling approach [14] to the simultaneous scaling of soil water retention and unsaturated hydraulic conductivity functions, yielding a single consistent set of scaling factors. In this analysis, the physically based simultaneous scaling factors are compared with those computed by the conventional scaling method.

2. Theory

Assuming a lognormally distributed soil pore radius (r) distribution, its probability distribution function (PDF) is defined by $f(\ln r) = \mathrm{d}S_e/\mathrm{d}\ln r$, where $S_e = (\theta - \theta_r)/(\theta_s - \theta_r)$ denotes the effective degree of water saturation, and $f(\ln r)$ is expressed by the normal distribution $N(\ln r_m, \sigma^2)$,

$$f(\ln r) = \frac{1}{\sigma\sqrt{2\pi}} \exp\left[-\frac{(\ln r - \ln r_m)^2}{2\sigma^2} \right], \tag{1}$$

where $\ln r_m$ and σ^2 are the mean and variance of log-transformed soil pore radius, $\ln r$, respectively. Hence, r_m is the geometric mean or median pore radius for which $S_e = 0.5$, assuming a lognormal pore-size distribution, and σ describes the width of the soil pore radius distribution. The concept of lognormally distributed pore size [13] is not new, and was introduced earlier [7,12]. Pore radius, r, is related to the soil capillary pressure head, h, by the capillary pressure function ($h > 0$ for unsaturated soils)

$$h = \frac{2\gamma \cos\beta}{\rho_w g r} = \frac{A}{r} \quad \text{or} \quad \ln h = \ln A - \ln r, \tag{2}$$

where γ is the interfacial tension (F L^{-1}), β the contact angle, ρ_w the density of water (M L^{-3}), and g is the acceleration of gravity (L T^{-2}), to yield an approximate value of $A = 0.15$ cm^2. This h notation is used throughout, instead of h denoting the matric potential head ($h < 0$ for unsaturated soils). Using Eq. (2), the soil water retention function is derived from Eq. (1), or

$$S_e(\ln h) = \frac{\theta - \theta_r}{\theta_s - \theta_r} = F_n\left[\frac{(\ln h_m - \ln h)}{\sigma} \right], \tag{3}$$

where $F_n(x)$ is the normal distribution function defined as

$$F_n = \frac{1}{\sqrt{2\pi}} \int_{-\infty}^{x} \exp\left(-\frac{x^2}{2} \right) \mathrm{d}x, \tag{4}$$

where $\ln h_m$ and σ are the mean and standard deviation of $\ln h$, respectively. The capillary pressure head h_m is related to the median pore radius r_m by Eq. (2). An alternative expression for the retention function given in Eq. (3) can be written as:

$$S_e(\ln h) = \frac{1}{2}\mathrm{erfc}\left(\frac{\ln h - \ln h_m}{\sigma\sqrt{2}} \right), \tag{5}$$

where erfc denotes the complementary error function. An extensive derivation of the foregoing physically based soil water retention model was presented by Kosugi [13].

2.1. Scaling of water retention curves

Based on the similar media concept, the scaling factor, α_i, is defined as ratio of a characteristic length, λ_i, of

soil sample i to the characteristic length, $\hat{\lambda}$, of a reference soil:

$$\alpha_i \equiv \frac{\lambda_i}{\hat{\lambda}}. \tag{6}$$

Assuming that pore-size distribution is an invariant quantity, Kosugi and Hopmans [14] defined the pore radius r as the microscopic characteristic length, so that Eq. (6) becomes

$$\alpha_i = \frac{r_i}{\hat{r}} \quad \text{or} \quad \ln \alpha_i = \ln r_i - \ln \hat{r}, \tag{7}$$

where r_i and $\hat{r}$ are the largest water-filled pore-radii for soil sample i, and the reference soil at equal effective water saturation, respectively. Since $r_{\mathrm{m},i}$ ($S_\mathrm{e} = 0.5$) is assumed as a suitable representative pore radius to characterize individual soil water retention curves, its value is selected as the macroscopic characteristic length scale [14], so that Eq. (7) becomes

$$\alpha_i = \frac{r_{\mathrm{m},i}}{\hat{r}_\mathrm{m}} \quad \text{or} \quad \ln \alpha_i = \ln r_{\mathrm{m},i} - \ln \hat{r}_\mathrm{m}. \tag{8}$$

Subject to the constraint that the geometric mean of the set of scaling factors is unity, i.e.,

$$\prod_{i=1}^{I} \alpha_i^{1/I} = 1.0 \quad \text{or} \quad \frac{1}{I}\sum_{i=1}^{I} \ln \alpha_i = 0,$$

it was shown by Kosugi and Hopmans [14] that $\ln \hat{r}_\mathrm{m}$ is equal to the arithmetic mean of all $\ln r_{\mathrm{m},i}$-values in the set. Subsequently, using the capillary equation (2), $\ln \hat{h}_\mathrm{m}$ and $\hat{\sigma}^2$ are computed from

$$\ln \hat{h}_\mathrm{m} = \mathrm{Mean}(\ln h_{\mathrm{m},i}) = \frac{1}{I}\sum_{i=1}^{I} \ln h_{\mathrm{m},i}, \tag{9}$$

$$\hat{\sigma}^2 = \mathrm{Mean}(\sigma_i^2) = \frac{1}{I}\sum_{i=1}^{I} \sigma_i^2, \tag{10}$$

where I denotes the number of soil samples in the set and the individual $\ln h_{\mathrm{m},i}$- and σ_i^2-values are determined from the fitting of Eq. (5) to individual soil water retention data to yield the soil water retention curve for soil sample i, $S_{\mathrm{e},i}$, or

$$S_{\mathrm{e},i}(\ln h) = \frac{1}{2}\mathrm{erfc}\left(\frac{\ln h - \ln h_{\mathrm{m},i}}{\sigma_i\sqrt{2}}\right). \tag{11}$$

Henceforth, the reference soil water retention curve was described by

$$\hat{S}_\mathrm{e}(\ln h) = F_\mathrm{n}\left(\frac{\ln \hat{h}_\mathrm{m} - \ln h}{\hat{\sigma}}\right) = \frac{1}{2}\mathrm{erfc}\left(\frac{\ln h - \ln \hat{h}_\mathrm{m}}{\hat{\sigma}\sqrt{2}}\right), \tag{12}$$

where $\ln \hat{h}_\mathrm{m}$ ($= \ln A - \ln \hat{r}_\mathrm{m}$) represents the mean $\ln h$-value for the reference soil. Accordingly, scaling factors for each soil sample, i, can be computed directly from

$$\alpha_i = \frac{\hat{h}_\mathrm{m}}{h_{\mathrm{m},i}} \tag{13}$$

or $\ln \alpha_i = \ln \hat{h}_\mathrm{m} - \ln h_{\mathrm{m},i}$. In [14] it was shown that the scaling factors determined from Eq. (13), while assuming a lognormal pore-size distribution model, are lognormally distributed.

2.2. Scaling of unsaturated hydraulic conductivity function

Based on the Miller and Miller scaling theory [17], scaling factors as determined from

$$K_i(S_{\mathrm{e},i}) = \alpha_i^2 \hat{K}(S_{\mathrm{e},i}) \quad \text{or} \quad \ln K_i = 2\ln \alpha_i + \ln \hat{K} \tag{14}$$

are identical as those obtained from soil water retention scaling as defined in Eq. (13) using $r_{\mathrm{m},i}$ as the macroscopic characteristic length scale for both hydraulic functions. Mualem [18] proposed the following predictive relative hydraulic conductivity model, which can be solved for $K_{\mathrm{r},i}$, provided that the soil water retention function, $S_{\mathrm{e},i}(h)$, is known:

$$K_{\mathrm{r},i} = \frac{K_i(S_{\mathrm{e},i})}{K_{\mathrm{s},i}} = S_{\mathrm{e},i}^{l}\left[\int_0^{S_{\mathrm{e},i}} \frac{\mathrm{d}S_{\mathrm{e},i}}{h} \Big/ \int_0^1 \frac{\mathrm{d}S_{\mathrm{e},i}}{h}\right]^2. \tag{15}$$

In other words, the relative hydraulic conductivity of soil sample i, $K_{\mathrm{r},i}$, is computed from $K_i(S_{\mathrm{e},i})$ and the saturated hydraulic conductivity, $K_{\mathrm{s},i}$ (L T^{-1}). In the predictive unsaturated hydraulic conductivity model, l describes the degree of connectivity between the water-conducting pores. In the subsequent analysis it is assumed that equal to $l = 0.5$ [18] although other values can be substituted if so warranted. Combining Eqs. (11) and (15) yields, the functional relationship between $K_{\mathrm{r},i}$ and $S_{\mathrm{e},i}$ (see Appendix A)

$$K_{\mathrm{r},i}(S_{\mathrm{e},i}) = S_{\mathrm{e},i}^{0.5}\left\{\frac{1}{2}\mathrm{erfc}\left[\mathrm{erfc}^{-1}(2S_{\mathrm{e},i}) + \frac{\sigma_i}{\sqrt{2}}\right]\right\}^2, \tag{16}$$

where erfc^{-1} denotes the inverse complementary error function. In the predictive unsaturated hydraulic conductivity model, l describes the degree of connectivity between the water-conducting pores. In the foregoing analysis it is assumed that $l = 0.5$ [18], although other values can be substituted if so warranted. Similarly, substitution of Eq. (12) into the Mualem model yields the hydraulic conductivity function for the reference soil:

$$\hat{K}_\mathrm{r}\left(\hat{S}_\mathrm{e}\right) = \frac{\hat{K}\left(\hat{S}_\mathrm{e}\right)}{\hat{K}_\mathrm{s}} = \hat{S}_\mathrm{e}^{0.5}\left\{\frac{1}{2}\mathrm{erfc}\left[\mathrm{erfc}^{-1}(2\hat{S}_\mathrm{e}) + \frac{\hat{\sigma}}{\sqrt{2}}\right]\right\}^2, \tag{17}$$

where $\hat{K}(\hat{S}_\mathrm{e})$ and $\hat{K}_\mathrm{s}$ denote unsaturated hydraulic conductivity (L T^{-1}) and saturated hydraulic conductivity

(L T^{-1}) of the reference soil, respectively, and $\hat{S}_e$ represents the soil water retention curve of the reference soil (Eq. (12)). Writing Eq. (14) for the saturated hydraulic conductivity and substitution of the constraint that the geometric mean of the set of scaling factors is equal to unity ($(1/I)\sum_{i=1}^{I} \ln \alpha_i = 0$) leads to the convenient result that the saturated hydraulic conductivity of the reference soil ($\hat{K}_s$) is equal to its geometric mean, or

$$\ln \hat{K}_s = \text{Mean}(\ln K_{s,i}) = \frac{1}{I}\sum_{i=1}^{I} \ln K_{s,i}. \quad (18)$$

Moreover, Eq. (14) written for the saturated hydraulic conductivity predicts that K_s is lognormally distributed since the log-transformed scaling factors, $\ln \alpha_i$, are normally distributed.

3. Material and methods

3.1. Experimental

To test the proposed simultaneous scaling theory, undisturbed soil samples were collected from 72 64 × 64 m^2 plots at two depths (25 and 50 cm) in a 40 ha field. This long-term research on agricultural systems (LTRAS) project is conducted at the Russell Ranch of the University of California [3,28] to study the long-term effects of irrigation and nitrate application to the sustainability of California agriculture. The field includes three different soil series: the Yolo (fine-silty, mixed, non-acid, thermic Typic Xerorothents), the Rincon (fine montmorillonitic, thermic Mollic Haploxeralfs), and the Brentwood (fine, montmorillonitic, thermic Typic Xerocrepts). Within each 64 × 64 m^2 plot, 8.25-cm inner diameter and 6-cm long soil cores were collected using a soil core sampler. The range of values of the main soil physical properties as obtained from these soil cores are [28]: bulk density, 1.22–1.66 g cm^{-3} ; organic matter, 0.43–1.63%; saturated hydraulic conductivity, 0.0002–17.79 cm h^{-1} ; saturated water content, 0.32–0.50 cm^3 cm^{-3}; sand (63–2000 ìm), 11–56%; silt (2–63 ìm), 34–80%; and clay (<2 ìm), 3–22%. For each core sample, soil hydraulic functions were measured using the multi-step outflow method in combination with parameter optimization [6,11].

The multi-step outflow method and parameter optimization code were slightly modified to improve the overall experimental outcome. Instead of a ceramic porous plate, we used a nylon membrane to support the core sample in the Tempe pressure cell. The low hydraulic resistance of the thin nylon membrane provides high flow rate and bubbling pressure (700 cm), thereby making it more suitable for parameter optimization. Pressure differences across the low resistance membrane are small so that there is no need to specify a hydraulic conductivity of the membrane in the combined flow and optimization code. Consequently, flow is not controlled by the membrane but solely by the soil, thereby improving the parameter optimization procedure. In addition, the optimization code provides for a time-dependent lower head boundary condition, to accommodate for the time-dependent water level in the burette, as measured with pressure transducers [29].

We assumed that the soil hydraulic properties are described by the lognormal pore-size distribution model, leading to the soil water retention and unsaturated hydraulic conductivity models, described by Eqs. (11) and (16), respectively. Whereas the saturated water content was fixed to its measured value, the residual water content (θ_r) for each sample i, $h_{m,i}, \sigma_i$, and $K_{s,i}$ were considered fitting parameters, to be optimized by the SFOPT software [29]. After parameter optimization of the soil hydraulic functions for each soil core, the data were divided into two subsets for each soil depth based on the magnitude of their optimized $h_{m,i}$-values, thereby grouping the soils into $\ln h_{m,i}$-values smaller or larger than 6.0. This grouping was conducted to satisfy the lognormality assumption of K_s and $h_{m,i}$ within each subset, as tested using fractile diagram analysis. Rather than the heuristic soil grouping based on the h_m-magnitude, we initially attempted to classify soils based on soil texture and related measured soil physical properties (bulk density, measured and optimized saturated hydraulic conductivity), but this analysis failed likely because of other non-measured soil attributes that control flow.

3.2. Scaling method

In the physically based (PB) scaling method, the functional parameters, $\ln \hat{h}_m$, $\hat{\sigma}^2$, and $\hat{K}_s$ for the reference soil water retention (Eq. (12)) and unsaturated hydraulic conductivity (Eq. (17)) for each subset (at 25 and 50 cm) were computed directly from Eqs. (9), (10), and (18) using the optimized soil core-specific parameters of the individual soil retention and unsaturated hydraulic conductivity functions. Scaling factors were directly calculated from the retention curve parameter, $h_{m,i}$, using Eq. (9). Subsequently, their values were applied to the K-scaling as well, using Eq. (14).

In the conventional scaling approach (C), the parameters, $\ln \hat{h}_m$, $\hat{\sigma}^2$, and $\hat{K}_s$ for the reference soil water retention (Eq. (12)) and unsaturated hydraulic conductivity functions (Eq. (17)) and scaling factor values were simultaneously estimated by a least squares fitting procedure provided in the Excel software [36], minimizing the residual sum of squared differences between the scaled mean curves and the scaled hydraulic data [4,10,14]. Defining appropriate weighting factors, the weighted root mean squared residuals (weighted RMSR) were minimized from

Weighted RMSR

$$= \frac{1}{\sigma_{S_e}} \left\{ \frac{1}{\sum_{i=1}^{I} J(i)} \sum_{i=1}^{I} \left[\sum_{j=1}^{J(i)} \left(S_{e,i}^{j} - \hat{S}_e(\alpha_i h^j) \right)^2 \right] \right\}^{1/2} + \frac{1}{\sigma_{\ln K}} \left\{ \frac{1}{\sum_{i=1}^{I} J(i)} \sum_{i=1}^{I} \left[\sum_{j=1}^{J(i)} \left(\ln K_i^j(S_{e,i}^j) - \ln \hat{K}(S_{e,i}^j) - 2 \ln \alpha_i \right)^2 \right] \right\}^{1/2}, \quad (19)$$

where $S_{e,i}^j$ is the jth effective water saturation of soil sample i with a jth capillary pressure head of h^j, $\hat{S}_e(\alpha_i h^j)$ the effective water saturation of reference soil obtained by substituting $h = \alpha_i h^j$ into Eq. (12), $\ln K_i^j$ is the natural logarithm of jth unsaturated hydraulic conductivity of soil sample i, with a jth effective water saturation of $S_{e,i}^j$, and $\ln \hat{K}(S_{e,i}^j)$ is the natural logarithm of unsaturated hydraulic conductivity of the reference soil at $S_{e,i}^j$. In this study, we used 11 arbitrarily selected j- classes within the applied external pressure range in the multi-step outflow experiment of 20, 40, 60, 80, 100, 200, 300, 400, 500, 600, and 700 cm. S_e-values selected for the scaling of individual soil water retention and unsaturated hydraulic conductivity data (both PB and C method) correspond with the capillary pressure head values, determined by these applied air pressure increments.

To allow for equal weighting between the retention and conductivity data normalizing parameters defined by the inverse of the standard deviations, σ_{S_e} and $\sigma_{\ln K}$, as computed from all data within each subset were selected [5]. In the fitting procedure, the geometric mean of scaling factors was constrained to unity, or,

$$\text{Mean}(\ln \alpha_i) = \frac{1}{I} \sum_{i=1}^{I} \ln \alpha_i = 0.$$

This was done to be consistent with the physically based scaling approach.

4. Results and discussion

4.1. Optimized individual soil hydraulic functions

The average of all fitting parameter values for both subsets and sampling depths are listed in Table 1 ($\hat{h}_m$, $\hat{\sigma}$, and $\hat{K}_s$). These parameters combined define the reference hydraulic functions from which the individual hydraulic functions are scaled by the physically based (PB) scaling method using Eqs. (13) and (14). The data clearly show that the two subsets for each soil depth are distinctively different regarding their $\hat{\sigma}^2$-values, indicating that this grouping resulted in classification of soils with distinct pore-size widths. That is, according to the selection of the pore-size distribution model for the soil water retention function, σ denotes the standard deviation of the pore-size distribution, with larger σ-values characterizing soils with a wider range in water-conducting pore radii (finer-textured soils). An even better illustration of the differences between the two subsets is presented in Fig. 1, where the apparent coarser-textured soils are

Table 1
Parameters for reference soil hydraulic function curves (PB – physically based scaling; C – conventional scaling)

Depth (cm)	Number of samples	Subset	$\ln \hat{h}_m$		$\hat{\sigma}^2$		$\ln \hat{K}_s$	
			PB	C	PB	C	PB	C
25	56	$\ln h_{m,i} < 6.0$	5.02	5.04	2.05	1.51	−2.27	−2.88
	16	$\ln h_{m,i} \geqslant 6.0$	7.49	7.19	7.00	5.59	−2.54	−3.55
50	49	$\ln h_{m,i} < 6.0$	5.17	5.19	2.06	1.35	−1.92	−2.71
	22	$\ln h_{m,i} \geqslant 6.0$	7.51	7.11	7.48	4.68	−2.17	−4.36

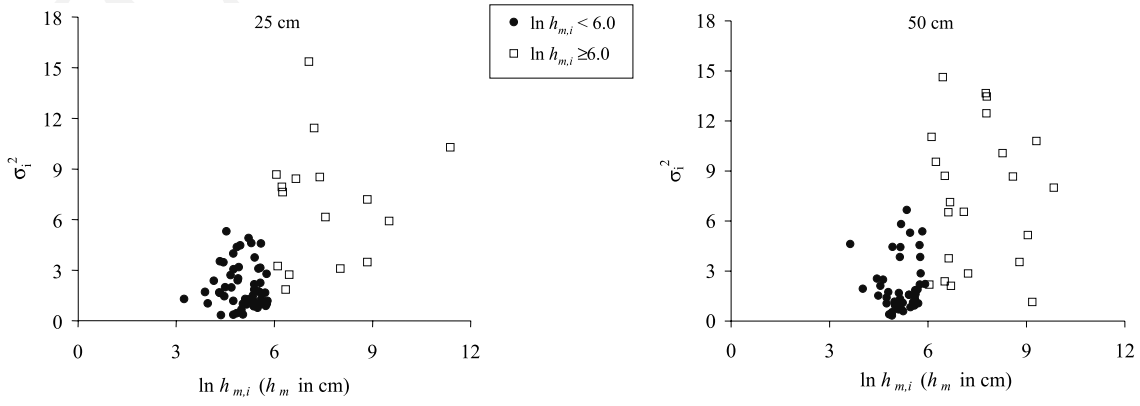

Fig. 1. Values of σ_i^2, versus $\ln h_{m,i}$ for both sampling depths.

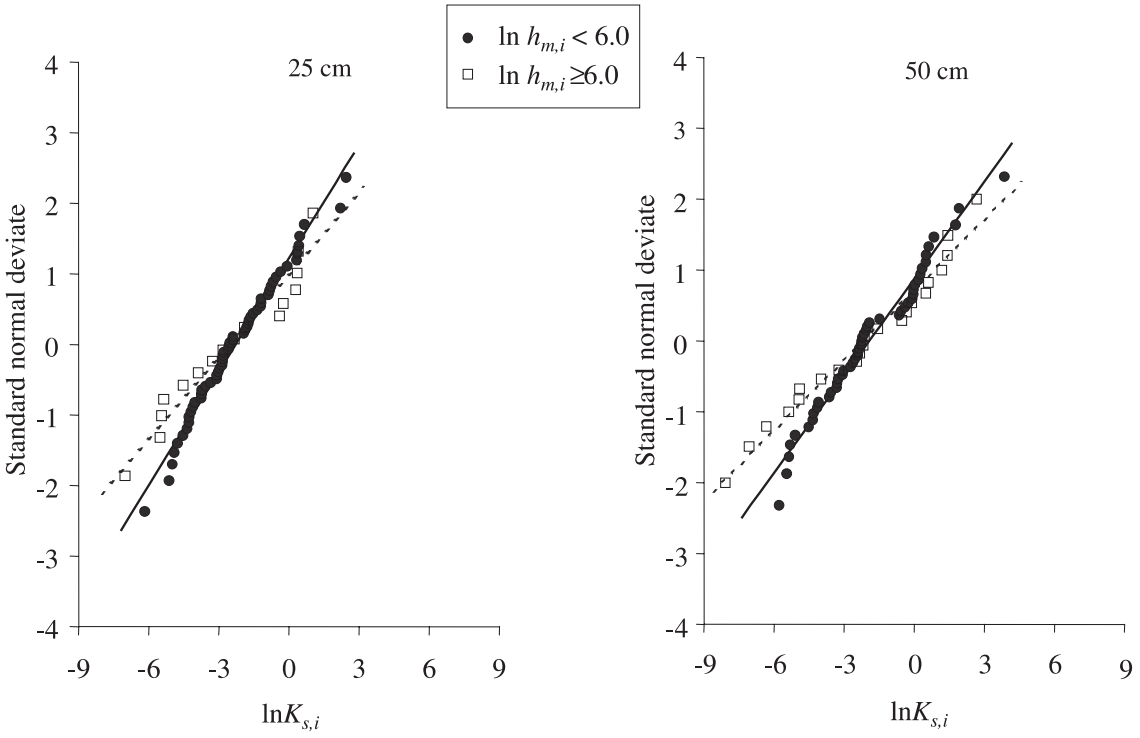

Fig. 2. Fractile diagram of the saturated hydraulic conductivity (ln $K_{s,i}$) for the both soil depths.

identified by ln $h_{m,i}$-values smaller than 6.0. We were, however, unsuccessful in using soil textural analysis to identify these two soil groupings a priori. Hence, other soil characteristics rather than soil texture alone, such as macroporosity and pore connectivity, may be needed to establish classes of hydraulically active soils. It may explain why many studies to relate soil water retention and/or unsaturated hydraulic conductivity with simple soil physical properties using pedotransfer function and regression analysis, have been partly unsuccessful [30,35].

In addition to the assumptions proposed by Kosugi and Hopmans [14] that lead to lognormally distributed scaling factor values, we have shown in Eq. (18) that the lognormal pore-size distribution model combined with the similar media scaling theory predicts that also the saturated hydraulic conductivity is lognormally distributed. Lognormality has been demonstrated by many experimental studies [15,19] and was also suggested by Kosugi and Hopmans [14] for lognormally distributed scaling factors. Lognormality of the optimized $K_{s,i}$ was analyzed by (1) construction of fractile diagrams (Fig. 2) and (2) applying the Kolmogorov–Smirnov test. This statistical test confirmed that the H_0-hypothesis of ln $K_{s,i}$ being normally distributed ($P = 0.2$) could not be rejected for each of the two subsets of each sampling depth. The standard normal deviate presented in the fractile diagrams is a linear transformation of all conductivity data so that they are normalized with a zero mean and unit variance, using normal probability tables. In the case of testing for lognormality, the saturated hydraulic conductivity data must fit along a straight line through the origin. The approximate linear fit to the data indicates that the selected h_m-criterion was adequate to yield subsets of lognormally distributed K_s-values.

Whereas in the PB approach, the mean value of ln $K_{s,i}$ (ln $\hat{K}_s$) for the reference soil was directly computed from optimized K_s-values of each soil sample i using Eq. (18), the ln $\hat{K}_s$ in the C-method was optimized by minimization of the residuals in Eq. (19). Since the saturated hydraulic conductivity is among the fundamental soil physical parameters controlling water flow in soil, K_s is expected to be correlated with the soil pore radius distribution parameters $h_{m,i}$ and σ_i^2. For example, coarse textured soils with large pores and narrow pore-size distribution will generally have larger conductivity values than the fine textured soils with wider pore-size distribution, at the same degree of saturation.

Indeed, when comparing ln $\hat{K}_s$-values in Table 1, we notice a lower saturated conductivity for the subsets with ln $h_{m,i} \geqslant 6.0$ (both soil depths), characterizing the finer-textured soils with larger values for the median ($\hat{h}_m$) of the reference soil. However, for the same h_m-value, Eq. (A.6) predicts that soils with larger σ-values (i.e., a wider pore-size distribution) have larger K_s, which contradicts our finding that apparent coarser-textured soils can be identified by smaller σ-values. As

indicated earlier, the soil saturated hydraulic conductivity depends not only on pore-size distribution, but also on the effective porosity and soil pore tortuosity and connectivity (the parameter l in Eq. (15)). Moreover, K_s is greatly affected by the presence of macropores.

4.2. Simultaneous scaling of soil hydraulic functions

The scaling results for the two subsets of the 25-cm soil depth based on PB scaling are presented in Figs. 3 and 4, respectively. In both figures, both the soil water retention and unsaturated hydraulic conductivity data are scaled simultaneously using scaling factors obtained from the median $h_{m,i}$-values only (Eq. (13)). Solid lines represent the mean hydraulic functions for the reference soil. As would be expected, the scaled soil water retention data for each soil sample coincide with the reference soil water retention curve at $S_e = 0.5$, corresponding with the median capillary pressure head values of 151.41 cm ($\ln h_{m,i} < 6.0$) and 1790.05 cm ($\ln h_{m,i} \geqslant 6.0$), respectively (Table 1). Scaling results for the other three subsets were similar to those shown in Figs. 3 and 4, and are therefore not presented.

The effectiveness of the simultaneous scaling was determined by comparison of the weighted root-mean squared residuals (WRMSR) of the unscaled and scaled soil water retention and unsaturated hydraulic conductivity data separately as well as combined. Values of WRSMR for both scaling methods and all four subsets are listed in Table 2. When comparing the residual values, it is noted that all subsets showed similar per-

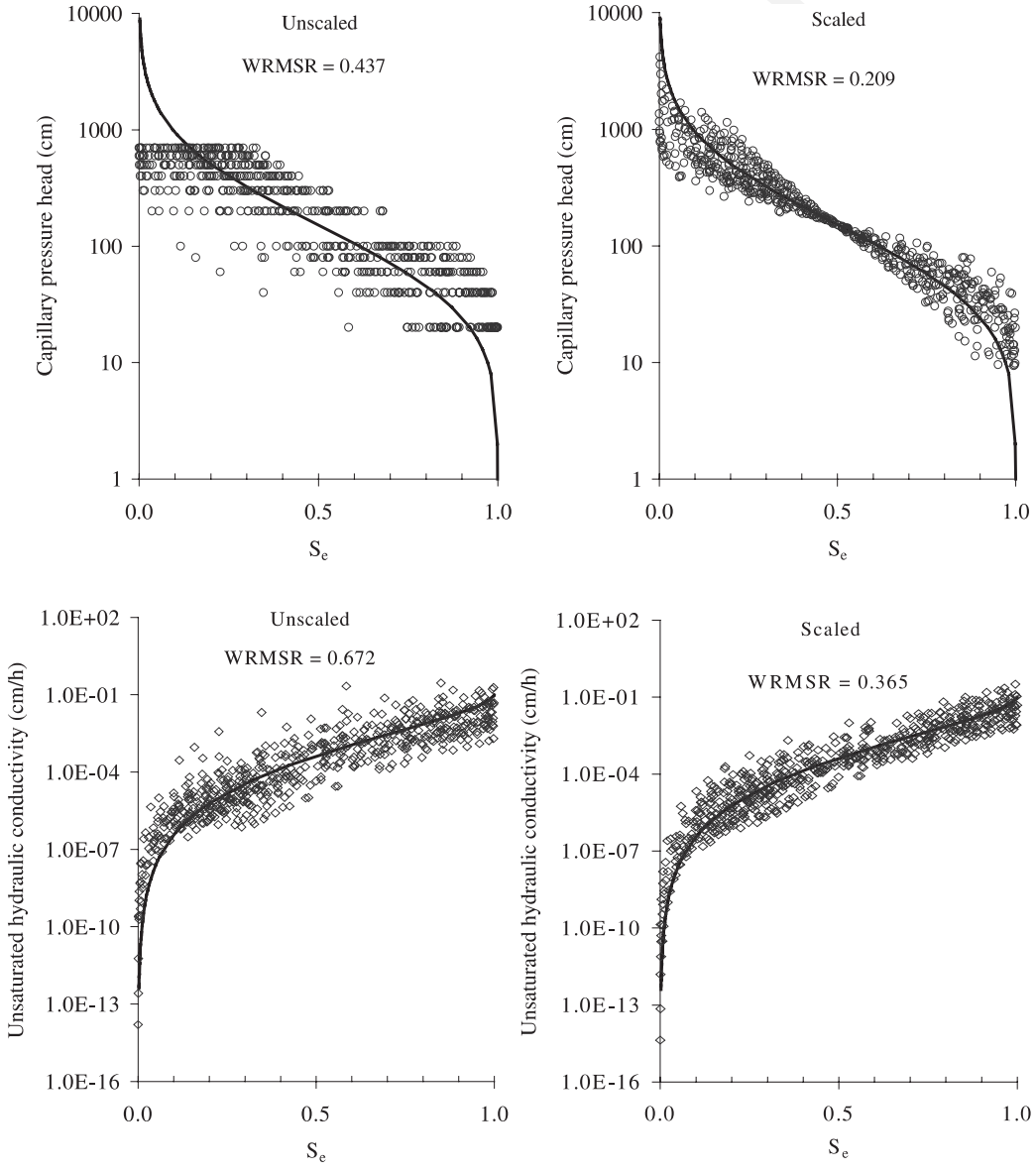

Fig. 3. Simultaneous PB scaling of subset $\ln h_{m,i} < 6.0$ at 25 cm.

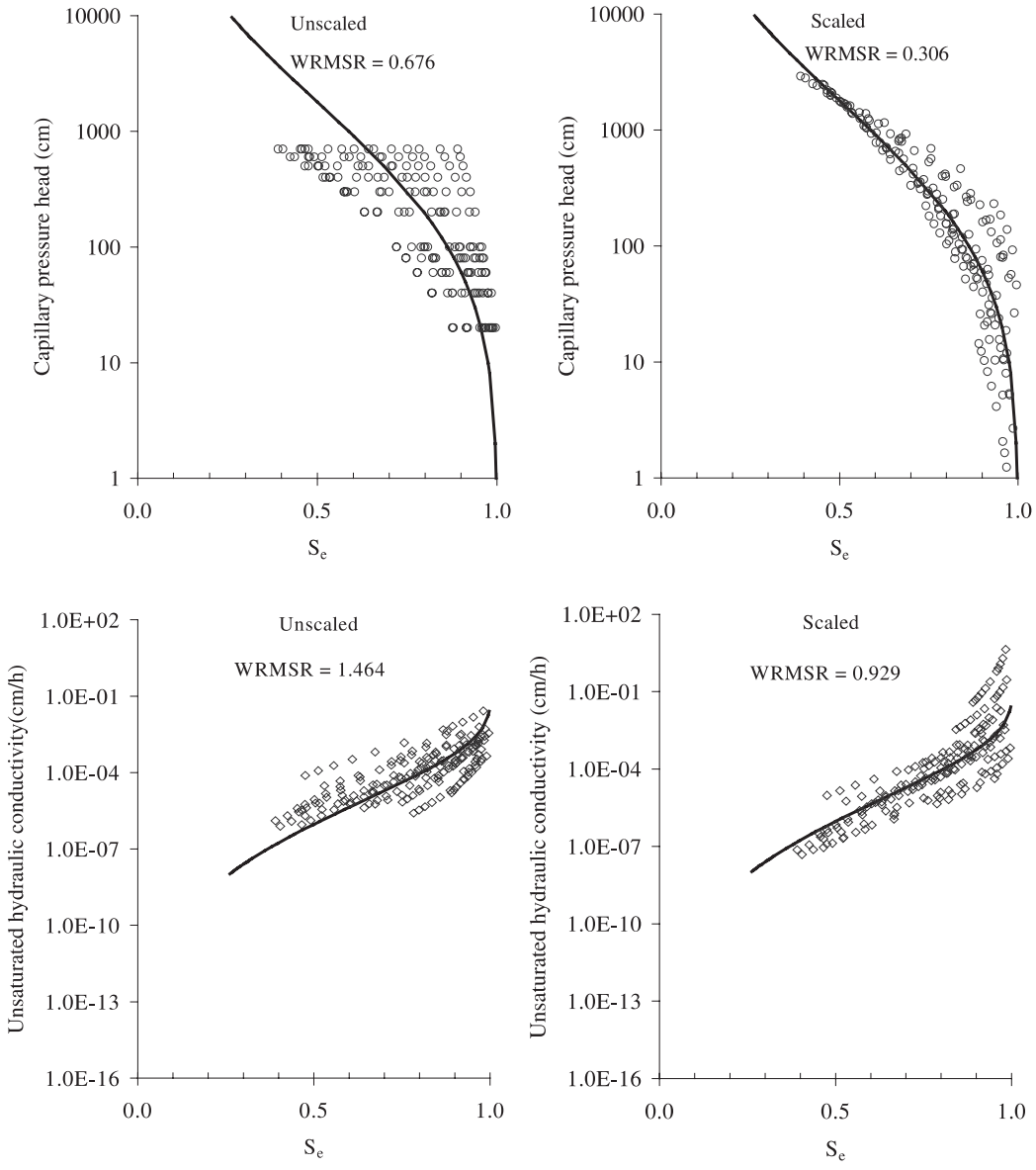

Fig. 4. Simultaneous PB scaling of subset $\ln h_{m,i} \geqslant 6.0$ at 25 cm.

Table 2
WRMSR and total reduction in PB and C scaling methods

Depth (cm)	Subset	Soil water retention				Hydraulic conductivity				Total reduction (%)	
		PB		C		PB		C			
		Unscaled	Scaled	Unscaled	Scaled	Unscaled	Scaled	Unscaled	Scaled	PB	C
25	$\ln h_{m,i} < 6.0$	0.437	0.209	0.446	0.235	0.672	0.365	0.658	0.265	48.214	54.704
	$\ln h_{m,i} \geqslant 6.0$	0.676	0.306	0.664	0.301	1.464	0.929	0.826	0.356	42.302	55.880
50	$\ln h_{m,i} < 6.0$	0.392	0.235	0.396	0.265	0.548	0.474	0.500	0.353	24.569	31.076
	$\ln h_{m,i} \geqslant 6.0$	0.592	0.414	0.585	0.299	1.089	0.837	0.566	0.395	25.631	39.692

formances with respect to scaling results and total reductions in WRMSR. In general, however, reductions in WRMSR were not so large as expected which suggests that the variances of the individual samples, σ_i^2 were quite different. As was illustrated in Fig. 2 [14], the presented scaling theory is based on the premise that the variance of the pore-size distribution of all considered soil samples are identical and equal to that of the scaled

mean reference curve. Differences in variances between soil samples is apparent also from inspection of Fig. 1, demonstrating that the range of variance values is at least as large or larger than the range of h_m-values. The smaller reduction in WRMSR for the 50-cm depth is caused by the lower measured variability of the soil hydraulic functions for that depth as compared to the spatial variability of the 25-cm depth. The slightly less effectiveness of the PB-approach is likely the result of scaling factors determined by the scaling of h at a single fixed S_e-value of 0.5 only, whereas the C-scaling method computes scaling factors by selecting the optimum S_e for each sample across the whole S_e-range, thereby being more flexible.

The differences in the mean hydraulic functions for the two subsets at the 25-cm soil depth are presented in Fig. 5. The shapes of the presented reference curves illustrate what was already inferred from comparison of the ln $\hat{h}_m$- and $\hat{\sigma}^2$-values of the two sets in Table 1. The dashed lines represent the hydraulic functions for the sampled soils characterized by ln $h_{m,i} \geqslant 6.0$ (finer-textured soil samples with large variation in pore sizes), whereas the solid lines describe the references curves for the coarser-textured soil subset with ln $h_{m,i} < 6.0$ and smaller pore-size variance. The comparison in Fig. 5 demonstrates that proper identification of different soil groupings is needed to increase the effectiveness of the similar media-based scaling approach.

Finally, the resulting scaling factor data sets were statistically analyzed for their distribution characteristics as well. These results are presented in Table 3, whereas the fractile diagrams of scaling factors for all four subsets and both scaling methods are shown in Fig. 6. Scaling factor distribution has consistently been found to be approximately lognormal [4,14,34]. Values for the slope and intercept of the fitted linear relationships in Fig. 6 characterize the statistical properties (mean and variance) of the lognormal scaling factor distributions. Hence, difference in slope distinguishes between scaling factor variability. Since the geometric

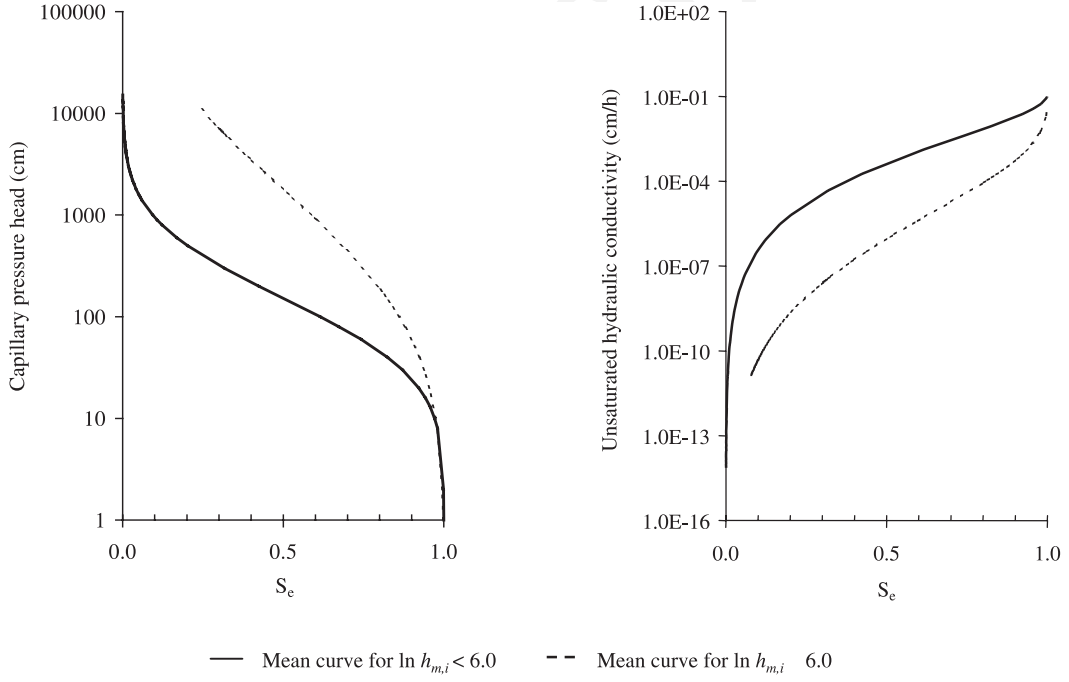

Fig. 5. Soil hydraulic function curves of subsets for reference soils at 25-cm depth.

Table 3
Statistical properties of scaling factors (Mean(ln α_i) = 0)

Depth (cm)	Number of samples	Subset	Mean (α_i)		Var(α_i)		CV (%)		Var(ln $h_{m,i}$)	Var($ln\,\alpha_i$)	
			PB	C	PB	C	PB	C		PB	C
25	56	ln $h_{m,i} < 6.0$	1.16	1.42	0.48	0.60	59.35	64.86	0.30	0.30	0.35
	16	ln $h_{m,i} \geqslant 6.0$	3.06	1.37	78.54	1.65	289.42	93.81	2.24	2.24	0.63
50	49	ln $h_{m,i} < 6.0$	1.12	1.15	0.32	0.44	50.53	57.55	0.23	0.23	0.29
	22	ln $h_{m,i} \geqslant 6.0$	2.01	1.22	12.34	0.74	174.57	70.21	1.40	1.40	0.40

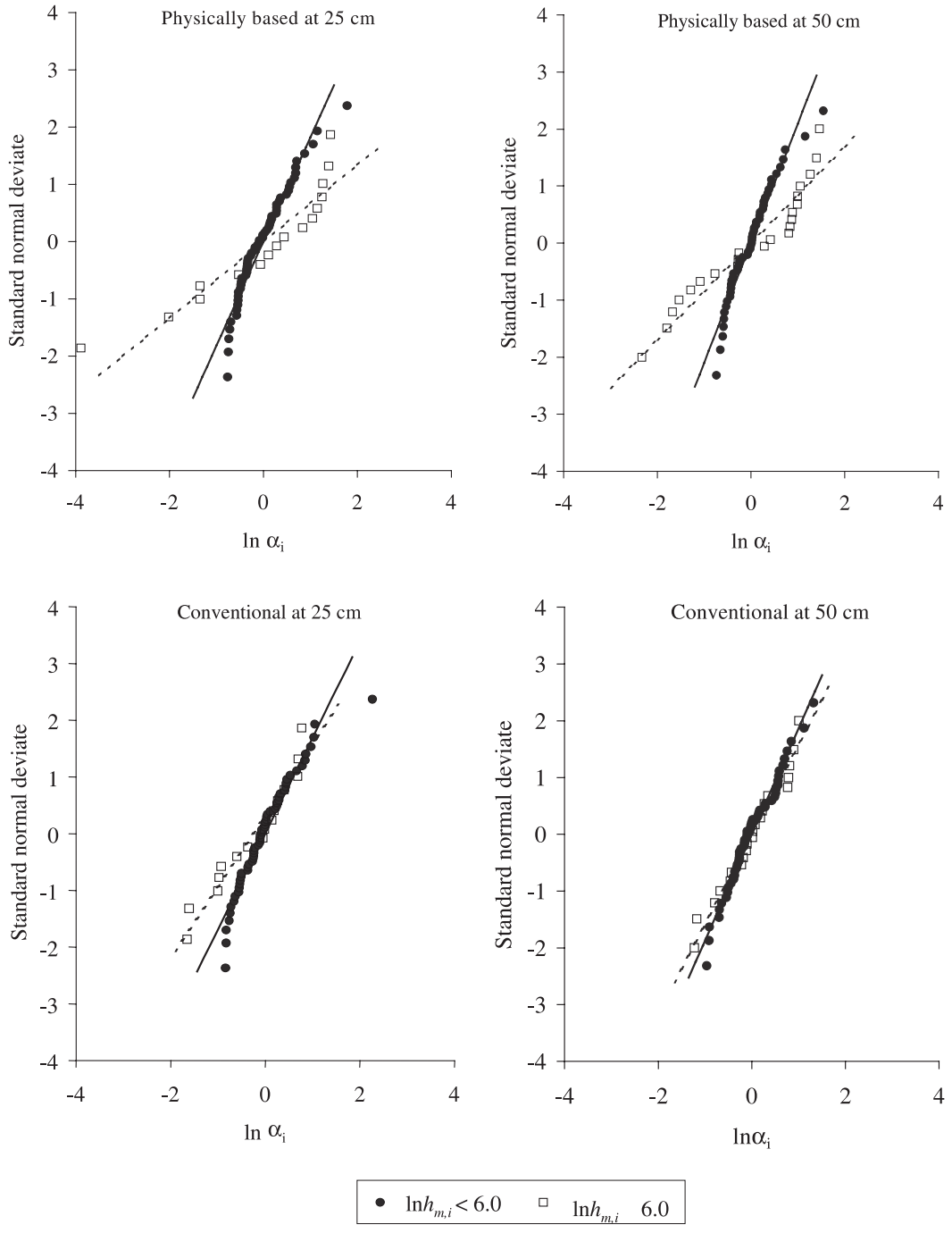

Fig. 6. Fractile diagrams of scaling factors distribution obtained by physically based and conventional method for all subsets of 25- and 50-cm soil depths.

mean of scaling factors is necessarily zero, linear regression was conducted with the intercept constrained to zero. From comparison of the fitted variance values in Table 3, it can be easily determined that the variance of the subset with $\ln h_{m,i}$-values larger than 6.0 (open squares in Fig. 6) is much greater than for the other subset. This is the case for both soil depths, but less so for the conventional scaling method. Specifically, for the subset $\ln h_{m,i} \geqslant 6.0$ of the PB method, the variance values between samples of the 25- and 50-cm soil depth are 2.24 and 1.40, respectively, and are much larger than any of the other reported values in Table 2 of Hendrayanto et al. [9]. These high variance values, as compared with the dataset of $\ln h_{m,i}$ smaller than 6.0 (solid dots), is caused by the larger variability of the measured soil hydraulic functions, as demonstrated by the larger $\mathrm{Var}(\ln h_{m,i})$-values in Table 3. Since the scaling factors are directly computed from the median capillary pres-

sure head, $\ln h_{m,i}$, the variance of $\ln \alpha_i$ obtained by the PB method must be equal to the variance of $\ln h_{m,i}$ [14]. It is also of interest to note that the large difference between sample variability of the datasets with $\ln h_{m,i} \geqslant 6.0$ corresponds with the largest $\hat{\sigma}^2$-values (with values of the within sample pore-size variability in the range of 7.0–7.5) of the same datasets (Table 1).

In addition to the results of the fractile diagrams, the lognormal behavior of scaling factors was also confirmed by the Kolmogorov–Smirnov test statistic ($P = 0.20$). Moreover, the large values for the coefficient of variation (CV) of scale factors in Table 3, are another indication that scaling factors are lognormal distributed [21]. The CV was calculated for the untransformed scale factors based on lognormal scaling factor distribution, yielding that $\mathrm{CV} = \sqrt{(e^{\sigma^2} - 1)} * 100\%$ [16,31].

5. Summary and conclusions

The theory of the physically based scaling method tested herein is based on the assumption that pore-size distribution as determined from the soil water retention curves is lognormally distributed. If in addition it is assumed that pores are geometrically similar, scaling factors computed from the median pore size or capillary pressure head can be directly applied to express variability of unsaturated hydraulic conductivity functions. Using an experimental data set of soil hydraulic functions, it is demonstrated that scaling factors as determined from individual soil retention curves can be directly used to scale unsaturated hydraulic conductivity data. It is shown that the physically based scaling theory predicts scaling factor and saturated hydraulic conductivity values that are log normally distributed as well.

To test the method, a total of 143 undisturbed soil samples at two soil depths (25 and 50 cm) were collected and soil water retention and unsaturated hydraulic conductivity curves were determined from parameter optimization using the multi-step outflow method. Beforehand, the hydraulic data of each soil depth were divided into two subsets to satisfy the lognormality assumptions. The physically based scaling method was compared with a conventional simultaneous scaling method where scaling factors were obtained by minimization of weighted residuals. With respect to the total reduction in WRMSR, both methods performed quite similarly, however, the PB method was slightly less effective, however, much more simple and direct.

We conclude that the physically based simultaneous scaling approach can be successfully used to express spatial variability of soil hydraulic functions.

6. Uncited reference

[2]

Appendix A

After substitution of Eq. (11), the numerator of the integral in Eq. (15) transforms to

$$\int_0^{S_{e,i}} \frac{dS_{e,i}}{h} = \frac{1}{\sigma\sqrt{2\pi}} \int_{\ln h}^{\infty} \exp(-\ln h) \times \exp\left[-\frac{(\ln h_{m,i} - \ln h)^2}{2\sigma_i^2}\right] d\ln h. \quad (A.1)$$

Substituting y for $(\ln h_{m,i} - \ln h)/\sigma_i$ yields

$$\int_0^{S_{e,i}} \frac{dS_{e,i}}{h} = \frac{1}{h_{m,i}\sqrt{2\pi}} \int_{-\infty}^{(\ln h_{m,i} - \ln h)/\sigma} \exp\left[y\sigma_i - \frac{y^2}{2}\right] dy \quad (A.2)$$

which after substitution of $z = (\sigma_i - y)/\sqrt{2}$ leads to

$$\int_0^{S_{e,i}} \frac{dS_{e,i}}{h} = \frac{\exp(\sigma_i^2/2)}{h_{m,i}\sqrt{\pi}} \int_{\frac{\sigma_i}{\sqrt{2}} - \frac{\ln h_{m,i} - \ln h}{\sigma_i\sqrt{2}}}^{\infty} \exp[-z^2]\, dz. \quad (A.3)$$

Hence, when written in terms of the complementary error function, the numerator of the hydraulic conductivity function becomes

$$\int_0^{S_{e,i}} \frac{dS_{e,i}}{h} = \frac{\exp(\sigma_i^2/2)}{h_{m,i}} \left\{\frac{1}{2}\mathrm{erfc}\left[\frac{(\ln h - \ln h_{m,i})}{\sigma_i\sqrt{2}} + \frac{\sigma_i}{\sqrt{2}}\right]\right\}. \quad (A.4)$$

Similarly, when applying the substitution rules to the denominator of Eq. (15), it transforms to

$$\int_0^{1} \frac{dS_{e,i}}{h} = \frac{1}{\sigma_i\sqrt{2\pi}} \int_{-\infty}^{\infty} \exp(-\ln h) \times \exp\left[-\frac{(\ln h_{m,i} - \ln h)^2}{2\sigma_i^2}\right] d\ln h, \quad (A.5)$$

which becomes

$$\int_0^{1} \frac{dS_{e,i}}{h} = \frac{\exp(\sigma_i^2/2)}{h_{m,i}}. \quad (A.6)$$

From Eq. (11), it follows that

$$\frac{\ln(h/h_{m,i})}{\sigma_i\sqrt{2}} = \mathrm{erfc}^{-1}(2S_{e,i}). \quad (A.7)$$

Finally, substitution of Eqs. (A.4), (A.6) and (A.7) in Eq. (15) allows direct computation of $K_{r,i}(S_{e,i})$ if the retention function, $S_{e,i}$, is known or

$$K_{r,i}(S_{e,i}) = S_{e,i}^{0.5}\left\{\frac{1}{2}\mathrm{erfc}\left[\mathrm{erfc}^{-1}(2S_{e,i}) + \frac{\sigma_i}{\sqrt{2}}\right]\right\}^2, \quad (A.8)$$

which is identical to Eq. (16).

References

[1] Ahuja LR, Naney JW, Nielsen DR. Scaling soil water properties and infiltration modeling. Soil Sci Soc Am J 1984;48:970–3.
[2] Brutsaert W. Probability laws for pore-size distributions. Soil Sci 1966;101:85–92.
[3] Chen J, Hopmans JW, Fogg GE. Sampling design for soil moisture measurements in small field trials. Soil Sci 1995;159(3):155–61.
[4] Clausnitzer V, Hopmans JW, Nielsen DR. Simultaneous scaling of soil water retention and hydraulic conductivity curves. Water Resour Res 1992;28(1):19–31.
[5] Clausnitzer V, Hopmans JW. Non-linear parameter estimation: LM_OPT. General-purpose optimization code based on the Levenberg–Marquardt algorithm. Land, Air and Water Resources Paper No. 100032, Davis, CA: University of California, 1995.
[6] Eching SO, Hopmans JW, Wendroth O. Unsaturated hydraulic conductivity from transient multi-step outflow and soil water pressure data. Soil Sci Soc Am J 1994;58:687–95.
[7] Gardner WR. Representation of soil aggregate-size distribution by a logarithmic-normal distribution. Soil Sci Soc Am Proc 1956;20:151–3.
[8] Granovsky AV, McCoy EL. Airflow measurements to describe field variation in porosity and permeability of soil macrospores. Soil Sci Soc Am J 1997;61(6):1569–76.
[9] Hendrayanto, Kosugi K, Mizuyama T. Scaling hydraulic properties of forest soils. Hydrol Process 2000;14(3):521–38.
[10] Hills RG, Hudson DB, Wiring PJ. Spatial variability at the Las Cruces Trench site. In: van Genuchten MTh, Leij FJ, Lund LJ, editors. Proceedings of the International Workshop on Indirect Methods for Estimating the Hydraulic Properties of Unsaturated Soils. Riverside, California; 1989 Oct 11–13.
[11] Hopmans JW, Simunek J, Romano N. Simultaneous determination of water transmission and retention properties – inverse modeling of transient water flow. In: Topp GC, Dane JH, editors. Methods of soil analysis. Part I. Third Edition American Society of Agronomy, Monograph No. 9, Madison, WI, 2001.
[12] Hopmans JW, Schukking H, Torfs PJF. Two-dimensional steady-state unsaturated water flow in heterogeneous soils with autocorrelated soil hydraulic properties. Water Resour Res 1988;24(12):2005–17.
[13] Kosugi K. Lognormal distribution model for unsaturated soil hydraulic properties. Water Resour Res 1996;32(12):2697–703.
[14] Kosugi K, Hopmans JW. Scaling water retention curves for soils with lognormal pore-size distribution. Soil Sci Soc Am J 1998;62(6):1496–505.
[15] Kutilek M, Nielsen DR. Soil hydrology. Cremlingen-Destedt, Germany: Catena Verlag; 1994.
[16] Jury WA, Russo D, Sposito G. The spatial variability of water and solute properties in unsaturated soil. II. Scaling models of water transport. Hilgardia 1987;55(4):33–56.
[17] Miller EE, Miller RD. Physical theory of capillary flow phenomena. J Appl Phys 1956;27:324–32.
[18] Mualem Y. A new model for predicting the hydraulic conductivity of unsaturated porous media. Water Resour Res 1976;12(3):513–22.
[19] Nielsen DR, Biggar JW, Erh KT. Spatial variability of field-measured soil–water properties. Hilgardia 1973;42:215–60.
[20] Nielsen DR, Hopmans JW, Reichardt K. An emerging technology for scaling field soil–water behavior. In: Sposito G, editor. Scale dependence and scale invariance in hydrology. Cambridge, UK: Cambridge University Press; 1998 p. 136–66.
[21] Parkin TB, Robinson JA. Analysis of lognormal data. In: Stewart BA, editor. Advances in soil science vol. 20. Springer: New York; 1992. p. 194–235.
[22] Russo D, Bresler E. Scaling soil hydraulic properties of a heterogeneous field. Soil Sci Soc Am J 1980;44:681–4.
[23] Simmons CS, Nielsen DR, Biggar JW. Scaling of field-measured soil–water properties. I. Methodology. Hilgardia 1979;47(4):77–102.
[24] Snyder VA. Statistical hydraulic conductivity models and scaling of capillary phenomena in porous media. Soil Sci Soc Am J 1996;60(3):771–4.
[25] Sposito G. Scaling invariance and the Richards equation. In: Sposito G, editor. Scale dependence and scale invariance in hydrology. Cambridge, UK: Cambridge University Press; 1998 p. 167–89.
[26] Sposito G, Jury WA. Miller similitude and generalized scaling. In: Hillel D, Elrick DE, editors. Scaling in soil physics: principles and applications. SSSA special publication number 25, Madison, Wisconsin; 1990.
[27] Tillotson PM, Nielsen DR. Scale factors in soil science. Soil Sci Soc Am J 1984;48(5):953–9.
[28] Tuli A, Hopmans JW, Rolston DE, Singer MJ. Soil quality assessment in irrigated agriculture: Influence of soil and water management on physical properties. In: Zabel A, Sposito G, editors. Soil quality in the California environment. Annual Report of Research Projects 1997–1998. Kearney Foundation of Soil Science, Division of Agriculture and Natural Resources, University of California, 1999.
[29] Tuli A, Hopmans JW, Harter T, Denton M. Multistep outflow experiment: from soil preparation to parameter estimation. Department of Land, Air, and Water Resources, University of California, Davis, 2000.
[30] Vereecken H. Derivation and validation of pedotransfer functions for soil hydraulic functions. In: van Genuchten MTh, Leij FJ, Lund LJ, editors. Proceedings of the International Workshop on Indirect Methods for Estimating the Hydraulic Properties of Unsaturated Soils. Riverside, California; 1989 Oct 11–13. p. 473–88.
[31] Warrick AW, Mullen GJ, Nielsen DR. Scaling field-measured soil hydraulic properties using similar media concept. Water Resour Res 1977;13(2):355–62.
[32] Warrick AW 1990. Application of scaling to the characterization of spatial variability in soils. In: Hillel D, Elrick DE, editors. Scaling in soil physics: principles and applications. SSSA special publication number 25, Madison, Wisconsin; 1990.
[33] Warrick AW. Spatial variability. In: Hillel D, editor. Environmental soil physics. New York: Academic Press; 1998. p. 655–76.
[34] Warrick AW, Nielsen DR. Spatial variability of soil physical properties in the field. In: Hillel D, editor. Applications of soil physics. New York: Academic Press; 1980. p. 319–44.
[35] Williams J, Ross P, Bristow K. Prediction of the Campbell water retention function from texture, structure, and organic matter. In: van Genuchten MTh, Leij FJ, Lund LJ, editors. Proceedings of the International Workshop on Indirect Methods for Estimating the Hydraulic Properties of Unsaturated Soils. Riverside, California; 1989 Oct 11–13. p. 427–42.
[36] Wraith JM, Or D. Nonlinear parameter estimation using spreadsheet software. J Nat Resour Life Sci Educ 1998;27:13–9.
[37] Zavattaro L, Jarvis N, Persson L. Use of similar media scaling to characterize spatial dependence of near-saturated hydraulic conductivity. Soil Sci Soc Am J 1999;63(3):486–92.